SPONSORED BY IEEE POWER ELECTRONICS AND INDUSTRY APPLICATIONS SOCIETIES

ECCE

ENERGY CONVERSION CONGRESS & EXPO

September 20–24, 2009

San Jose, CA DoubleTree Hotel

FIRST ANNUAL 2009

IEEE Energy Conversion Congress & Expo

TUTORIALS, TECHNICAL SESSIONS, EXHIBITS, INDUSTRIAL SEMINARS

Conference Management ECCE 2009 2025 M Street, NW, Suite 800 Washington DC, 20036 Phone: (202) 973-8744 Email: ecce@courtesyassoc.com Website: www.ecce2009.org

Exhibit Services Drayage and Decorating—Freeman • 3323 11135 North Suite 120 • San Antonio, TX 78219 • Phone: 210.227.0341

Magnetic Guidance of the Mover in a Long-Primary Linear Motor

Phong C. Khong
Student member, IEEE
Technical University Darmstadt
Karolinenplatz 5
64289 Darmstadt
phong@srt.tu-darmstadt.de

Roberto Leidhold
Member, IEEE
Technical University Darmstadt
Karolinenplatz 5
64289 Darmstadt
leidhold@srt.tu-darmstadt.de

Peter Mutschler
Member, IEEE
Technical University Darmstadt
Karolinenplatz 5
64289 Darmstadt
pmu@srt.tu-darmstadt.de

Abstract -- **Modern in-plant transport and handling systems benefits from using long-primary linear motors. To improve these systems, the lateral guidance of the vehicle is performed by magnetic forces instead of a mechanical guiding assembly. In this paper, an active guiding system is presented for PM-synchronous linear motors with long and double-sided primary. The air-gap and the yaw angle are controlled while a simple wheel-rail system fixes the vertical displacement. Each side of the primary is supplied by its own inverter allowing the necessary degree of freedom to control the air-gap and yaw angle in addition to the thrust. With this arrangement, the mover can be kept passive avoiding any energy transmission system to it. Experimental tests were performed on a laboratory prototype. The experimental results show good dynamic performance that in turn provides stiffness in the guidance.**

Index Terms- **Linear synchronous motors, Magnetic bearings, Permanent magnet motors.**

I. INTRODUCTION

Linear drives provide new solutions for material transportation and processing in the manufacturing industry. Instances of application can be found for stretching of plastic films [1] or in material handling [2]-[4].

For these applications, the linear motor is typically with stationary long primary and a short moving secondary [4]. As the secondary part is passive, no energy transmission is required between the moving and stationary part, avoiding the use of brushes or inductive transmission. The motor type best suited for the mentioned applications is the synchronous one with permanent magnets, because of its higher efficiency, compactness, but most important because it allows a higher air-gap.

In the usual approach, the linear motor is only used for thrust force production. The guidance is usually implemented by a mechanical assembly. The guidance constrains the movement to the longitudinal displacement, fixing the lateral and vertical displacement, yaw, roll and pitch. Such a mechanical assembly can be complex and source of high friction. It becomes even more complex when the track is non-straight as for instance in curvilinear conveyor systems.

Several proposals can be found in the literature to substitute the mechanical guidance, partially or totally, by magnetic guidance. Magnetic levitation will be considered here as the guidance for vertical displacement and pitch. Magnetic bearings and bearing-less motors are the rotative counterparts of magnetic guidance, and several methods derive from them.

By using electro-dynamic levitation or null flux coils [5], passive magnetic guidance can be provided for one or more degrees of freedom. The drawback is the dependence on the longitudinal speed i.e. it does not provide guidance at standstill. The superconducting magnetic bearing [6] is a passive guidance method that works even in standstill, requiring however a cryogenic system.

Different methods for active magnetic guidance can be found proposed, among others, in [7]-[10]. These methods rely on using separate windings for the guidance and propulsion. These windings are located in the mover, requiring therefore an energy transmission system to the mover. In [11], the windings used for propulsion, i.e. motor's primary, are also used for guidance (levitation). As the primary is in the mover, here again an energy transmission system is required. The proposal of [12] is a complete guiding system for a long primary linear motor. The air-cored primary is placed in the guideway and is used for propulsion as well as for the guidance. In this case, the mover does not need a power supply besides for the position sensors. The magnitude, angle and zero-sequence of the currents supplied to each primary-side are the manipulated variables to control the six degrees of freedom required for the control of longitudinal movement and the guidance.

In this paper, an active guiding system is presented for PM-synchronous linear motors with long and double-sided primary. The lateral displacement and the yaw angle are controlled while a simple wheel-rail system fixes the vertical displacement. This combination of magnetic and mechanical guidance offers a good tradeoff among the complexity of the control, actuators and mechanics, when considering industrial applications. To allow multiple vehicles traveling simultaneously and independently on the guideway (each vehicle is controlled by an individual part of the guideway), the double side primary is separated into segments. With that structure, flexible-operating methods can be implemented. That is very useful in process integrated material handling where different speeds of material carriers in each processing station are necessary. Another advantage of segmented structure is the energy saving. The power is supplied only to the segment or the two consecutive segments in which the vehicle runs over. In one segment, each side of the primary is

supplied by its own inverter, allowing the necessary degree of freedom to control the lateral position and yaw angle in addition to the thrust. With this arrangement, the mover can be kept passive avoiding any energy transmission system to it (besides for the sensors). Unlike [12], here a standard three-phase iron-cored primary section is used. In addition, the direct and quadrature current components in a field-oriented reference frames are the manipulated variables instead of the magnitude and angle.

II. MODEL OF THE LINEAR MOTOR

The machine considered for the proposed guidance system is a long-primary (guideway) with a short-mover (vehicle) linear motor. A cross section of the system is shown in Fig. 1.

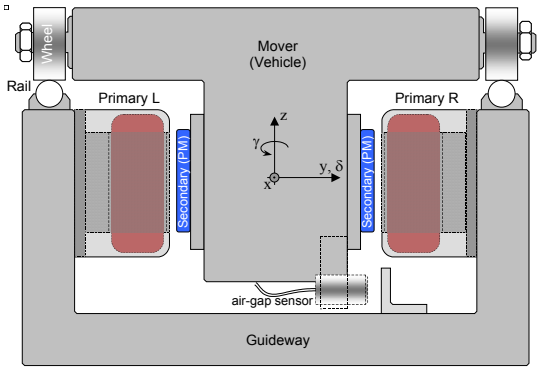

Fig. 1. Cross section of the long-primary linear motor.

The vehicle has two secondary sections mounted opposite each other in the lower part of the vehicle. Each secondary section has a permanent magnet (PM) array fastened on a back iron plate. The iron-cored primary sections are installed along both sides of the guideway. Each primary side section is fed separately to generate lateral and propulsive force on the correlative secondary section. In the case that the vehicle moves over two segments, lateral and propulsive forces are generated by four primary sections. With that structure the movement in y-axis can be controlled by the differential lateral forces, the rotation and x position of the mover are controlled respectively by the difference and total of propulsive forces. The movement in the z-axis is constrained by the rail-wheel system. The lateral displacement i.e. in the y-axis, is named as δ , and the yaw angle γ .

In order to compute the forces of the motor, a sinusoidal winding distribution is assumed and is modeled by a thin current layer as presented in Fig. 2. In the same way, the PMs are assumed producing a sinusoidal flux distribution along the mover's length. The fundamental harmonic component of PM equivalent current density and the primary line current density are presented in static and moving frame as follow

$$A_{1PM}(x_m) = \frac{4}{\tau} M_{PM} \sin(\frac{\pi\tau_p}{2\tau}) \cos(\frac{\pi}{\tau} x_m) \quad (1)$$

$$A_{1a}(x_s, t) = \frac{3\sqrt{2} N_1 I_a k_{\omega 1}}{\tau p} \cos(\omega t + \frac{\pi}{\tau} x_s) \quad (2)$$

Present in synchronous moving frame

$$A_{1a}(x_m) = \frac{3\sqrt{2} N_1 I_a k_{\omega 1}}{\tau p} \cos(\frac{\pi}{\tau} x_m - \theta_0) \quad (3)$$

Where $H_{PM} = H_c d_M$ is the magnetomotive force (MMF) of the PM per pole, I_a is armature phase current, p is number of pole pairs per one stator segment, N_1 is number of series turns per phase. The parameter $k_{\omega 1}$ is the winding factor, $\omega = 2\pi f$ is the angular frequency, τ is the pole pitch, τ_p is the magnet width, x_0 is the displacement between stator's coordinates and PM's coordinate, $\theta_0 = \pi x_0 / \tau$ is the phase angle between the primary and secondary equivalent currents.

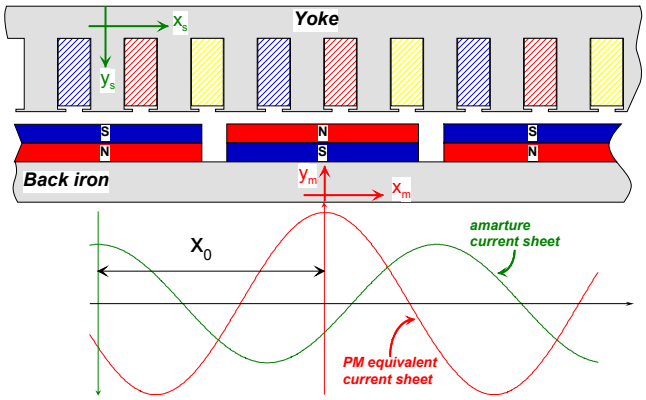

Fig. 2. Sinusoidal flux distribution

In the case that the air-gap is constant along the mover's length, the force analysis yields closed equations [13]. However, in the case that a yaw angle is considered, the air-gap is not constant along the mover's length and a closed expression of the forces are not possible anymore. In this case, the forces must be computed numerically for a given motor.

Because of the mechanical limitation, the yaw angle is kept small. So, it will be neglected ($\gamma = 0$) in order to simplify the force calculations. By numerical calculation and the practical measurement, it can be proven that the force and torque caused by the yaw angle are small in comparison with the others. In company with the assumption of sinusoidal winding and flux distribution, the propulsive and normal forces are calculated by integrating the force components along the vehicle length. The obtained results are the propulsive and normal forces depending nonlinearly on primary current (i_a), vehicle displacement (θ_0) and the lateral displacement (δ).

$$F_N = \left\{ K_1 - \frac{3}{2} \cos(\theta_0) i_a \left(K_2 i_a + K_3 \right) \right\} \frac{1}{(\delta + d_M)^2} \quad (4)$$

$$F_T = K_4 \frac{i_a \sin(\theta_0)}{\delta + d_M} \quad (5)$$

Where K_1, K_2, K_3, K_4 are constants of the motor; d_M is the magnet thickness.

To be able to use the field-oriented control method, (4) and (5) must be represented by dq currents as defined by:

$$i_d = i_a.\cos(\theta_0) \quad (6)$$

$$i_q = i_a.\sin(\theta_0) \quad (7)$$

Moreover, each primary side is supplied by an independent inverter. So, the propulsive forces and thrust forces generated by independent controlled primaries can be presented as below

$$F_{NL} = \left\{K_1 - \frac{3}{2}\left(K_2 i_{dL} i_{aL} + K_3 i_{dL}\right)\right\} \frac{1}{\left(d_M + \delta\right)^2} \quad (8)$$

$$F_{NR} = \left\{K_1 - \frac{3}{2}\left(K_2 i_{dR} i_{aR} + K_3 i_{dR}\right)\right\} \frac{1}{\left(d_M - \delta\right)^2} \quad (9)$$

$$F_{TL} = K_4 \frac{i_{qL}}{d_M + \delta} \quad (10)$$

$$F_{TR} = K_4 \frac{i_{qR}}{d_M - \delta} \quad (11)$$

Where F_{NL}, F_{NR}, F_{TL} and F_{TR} are correlatively normal forces and thrust forces of left and right side.

The nonlinear equations (8)-(11) are difficult to use in order to implement the control method. For calculating a simpler controller, these equations must be linearized. As a result of the linearization for both sides, the forces acting on the mover are functions of the left and right side d-axis currents (i_{dL}, i_{dR}), q-axis currents (i_{qL}, i_{qR}), lateral position δ and yaw γ. From calculated results, an approximation can be obtained:

$$F_x = i_x K_x + i_\gamma K_{x\delta} \delta \quad (12)$$

$$F_\delta = i_\delta K_\delta + F_{\delta p}(\delta, \gamma, i_x, i_\delta, i_\gamma) \quad (13)$$

$$T = i_\gamma K_\gamma + i_\delta K_{\gamma\delta} \delta \quad (14)$$

where K_x, K_δ, K_γ, $K_{x\delta}$, $K_{\gamma\delta}$ are constants of the motor; $F_{\delta p}$ is the force resulting from the attraction between the magnets and the primary iron; i_x, i_δ and i_γ are the propulsion, lateral force and yaw torque producing currents, respectively, related with the primary currents as follows:

$$\begin{cases} i_{qL} = i_x + i_\gamma, & i_{qR} = i_x - i_\gamma \end{cases} \quad (15)$$

$$\begin{cases} i_{dL} = -\frac{i_\delta}{2}, & i_{dR} = \frac{i_\delta}{2} \end{cases} \quad (16)$$

The force terms $F_{\delta p}$, $i_\gamma K_{x\delta}\delta$ and $i_\delta K_{\gamma\delta}\delta$ are dependent on the position, dq current (i_d, i_q) of left and right primaries, and can be considered as perturbations. In other words, the control algorithm can work without compensating those values, however at the cost of a poorer performance. To obtain a higher control quality, they will be compensated in the control algorithm.

The motion equations are:

$$\frac{d\,v}{dt} = \frac{F_x}{M}, \quad \frac{d\,\varepsilon}{dt} = \frac{F_\delta}{M}, \quad \frac{d\,\omega}{dt} = \frac{T}{J} \quad (17)$$

$$\frac{d\,x}{dt} = v, \quad \frac{d\,\delta}{dt} = \varepsilon, \quad \frac{d\,\gamma}{dt} = \omega \quad (18)$$

With M and J are the mass and moment of inertia of the mover, respectively.

III. PROPOSED CONTROL METHOD

Based on the approximated model (12)-(18), considering all values $F_{\delta p}$, $i_\gamma K_{x\delta}\delta$ and $i_\delta K_{\gamma\delta}\delta$ as the perturbations, and a current controlled inverter, it is proposed to use a standard cascaded controller for each degree of freedom:

$$i_x^* = k_{pv}(v^* - v) + \frac{k_{pv}}{T_i}\int_0^t (v^* - v)\,dt \quad (19)$$

$$i_\delta^* = k_{p\varepsilon}(\varepsilon^* - \varepsilon) + \frac{k_{p\varepsilon}}{T_i}\int_0^t (\varepsilon^* - \varepsilon)\,dt \quad (20)$$

$$i_\gamma^* = k_{p\omega}(\omega^* - \omega) + \frac{k_{p\omega}}{T_i}\int_0^t (\omega^* - \omega)dt \quad (21)$$

$$v^* = k_{px}(x^* - x) \quad (22)$$

$$\varepsilon^* = k_{p\delta}(\delta^* - \delta) \quad (23)$$

$$\omega^* = k_{p\gamma}(\gamma^* - \gamma) \quad (24)$$

The parameters of the controller (k_{pv}, $k_{p\varepsilon}$, $k_{p\omega}$, T_i, k_{px}, $k_{p\delta}$ and $k_{p\gamma}$) are determined by the symmetrical optimum criteria using the approximated model [14]. With these parameters, the stability of the equilibrium points was proved in a wide set of positions, using the complete model, by numerical analysis.

The reference values for lateral position δ^* and yaw angle γ^* are set to zero, while the reference for the longitudinal position x^* is determined by the task assigned to the system.

In order to improve control quality, a compensating control method was implemented to reduce the perturbation of lateral force $F_{p\delta}$. The proposed reference current for delta control becomes

$$i_{\delta C}^* = i_\delta^* - \frac{F_{\delta p}(\delta, i_x, i_\delta, i_\gamma)}{K_\delta} \quad (25)$$

The block control diagram is show on Fig. 3.

IV. EXPERIMENTAL SETUP AND RESULTS

In order to test the proposed system, a prototype based on the diagram of Fig. 1 was implemented. The prototype was built on aluminum profiles and standard commercial stators and magnets. In Fig. 4, a picture of the prototype is shown. In Table 1 the most important parameters are given.

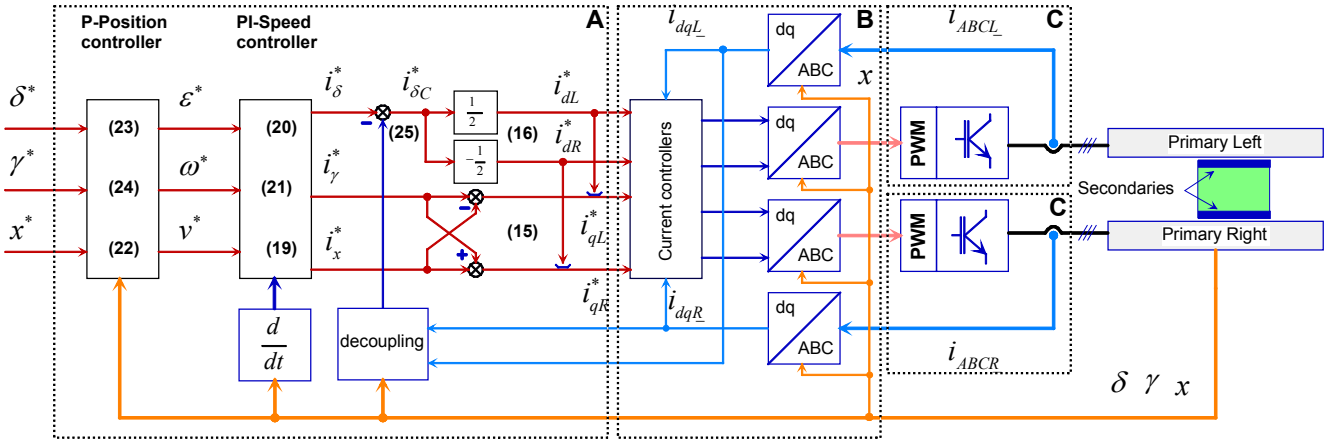

Fig. 3. Control block diagram.
A: Three axes controller B: Current control and communication C: Inverters

TABLE 1
MAIN PARAMETERS OF THE LINEAR MOTOR.

Primary length	542 mm
Secondary length	144 mm
Lateral displacement range	3 mm
Pole pitch	36 mm
Rated current	2.9 A rms
Maximal current	21.3 A rms
Rated thrust force	210 N
Mass of the mover	5.7 Kg
Moment of inertia of the mover	0.038 Kg.m2

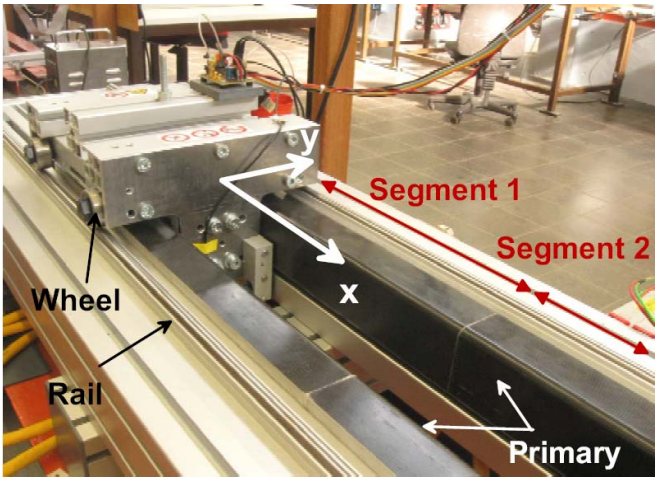

Fig. 4. Prototype of the linear motor with magnetic guidance

Each primary side of a segment is supplied with its own inverter, with a 5 kHz switching frequency. All inverters are controlled by one PC-based controller using the RTAI-Linux real time operating system. The control algorithm operates at a sampling frequency of 10 kHz. In each moment, two (or four in the case that the vehicle runs over two segments) inverters are controlled to supply the power for the stators of the correlative segments. The other inverters are set at standby status. The position information is used to select which inverters must operate. The communication between the control PC and the inverters is implemented by self-developed interface cards with a 16 bits parallel bus. Each card mounted on an inverter. Besides the communicating function, the interface cards also have PWM signal generating and AD converting functions. They generate the PWM signals for the inverters and send the AD converted signals of the three phase currents to the control PC [15]. The block diagram of experimental system is showed in Fig. 14.

The longitudinal position is measured by a linear encoder with a magnetic scale and a magneto resistive sensor. The resolution of the encoder is 5 µm. Two analog proximity sensors are placed at the ends of the mover. The lateral position is obtained from the average of both sensors, and the yaw angle from the difference. These sensors have a bandwidth of 10 kHz.

A. Control performance experiment

Experiment results were obtained with the described experimental setup. A test was performed to check the control performance of the proposed method on the prototype system. The test is implemented to control the three-degree of freedom simultaneously. In Fig. 5, the system is started from a rest position with the highest absolute value of delta ($-\delta_{max}$), i.e. the magnets of the mover stuck at the right stator. At t = 0.1s, the references δ^*, γ^* are set to zero and x* = 100mm (mover centered and parallel to the guideway). At t = 0.4s, the reference for the longitudinal position is set to x* = 300mm. At t = 0.9s, the reference γ^* is established to a new value of 0.5 mrad.

To identify the differences between standard cascade controller, considering the force terms $F_{\delta p}$, $i_\gamma K_{x\delta}\delta$ and $i_\delta K_{\gamma\delta}\delta$ as the perturbations, and the compensated cascade controller, the experiments were implemented in two cases: without and with decoupling. The measured lateral position,

yaw angle and longitudinal position of the first case are shown in Fig. 5 as a function of time. The results of the second (decoupling compensation) case are shown in Fig. 6.

From the experiment results shown in Fig. 5 and Fig. 6 it is easy to recognize that the control system can work without compensation but the control quality is poor. Especially at the beginning when the lateral displacement δ is high, the perturbation $F_{\delta p}$ effects strongly to the control quality. The control quality is much better when the compensation is used.

The current i_d, used for delta control, and the current i_q, used for gamma and x control, are components of the same current vector. The magnitude of the current vector must be limited, by limiting each of its components. On other hand, the attractive force between the primary iron-core and the PM (lateral force) is very high. Therefore, in the control algorithm, a higher priority is given to the current component for delta control (i_d) while limiting the other component (i_q). That is why at t=0.1s delta is controlled well and gamma oscillates a short time. However, at t=0.9s when the vehicle is in the middle of the guideway, the lateral force is balanced between left and right side. Consequently, i_d is small at that time and a step in gamma reference γ^* is responded with higher quality.

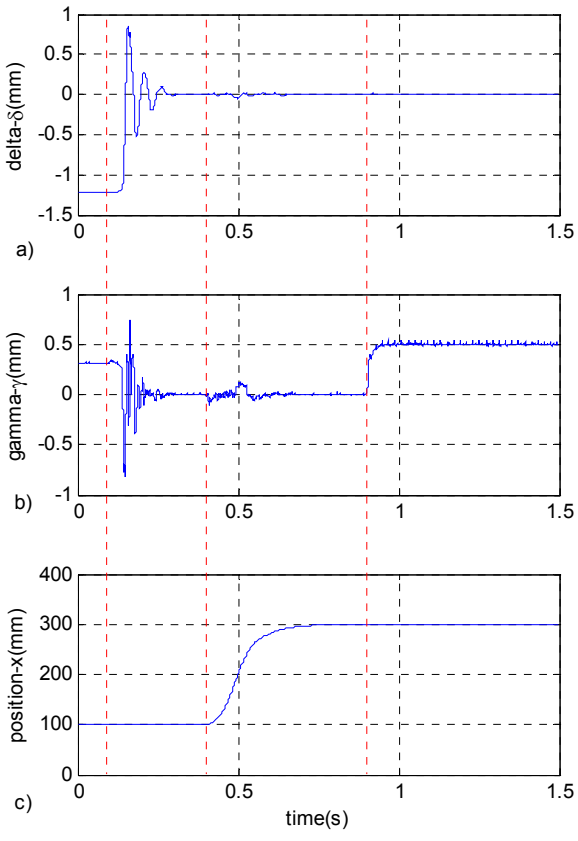

Fig. 5. Startup and movement control (experimental); lateral position, yaw angle and longitudinal position without compensation

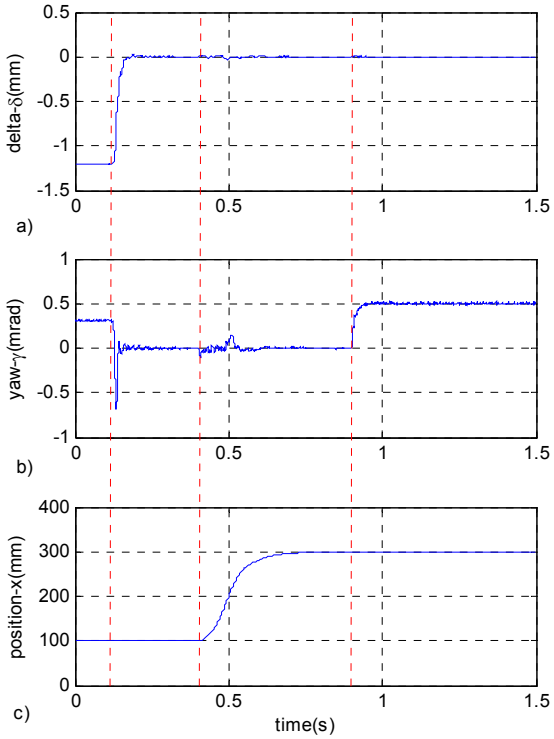

Fig. 6. Startup and movement control (experimental); lateral position, yaw angle and longitudinal position with compensation

During the movement of the vehicle from 100 to 300mm, there is some disturbance in gamma and delta. The ability to startup from the rest position shows that the controller is able to compensate all couplings between delta and gamma control loops.

The resulting measurements of current i_d and i_q are presented in Fig. 7 and Fig. 8 as the function of time. In Fig. 7.a-b, 8.a-b i_{dL} and i_{dR} are symmetrical. They are very high when the delta position of the vehicle is controlled from the rest position to zero. When the vehicle is on the middle of the guide way, the required i_d is much smaller (almost zero). The currents i_{qL} and i_{qR}, shown in Fig. 7.c-d and Fig. 8.c-d, generate the thrust force and rotating torque for the vehicle. Consequently, when the vehicle is moving or rotating, the total and difference of i_{qL} and i_{qR} change correlatively.

In Fig. 9 and Fig. 10 the corresponding currents for lateral force (i_δ), yaw torque (i_γ) and propulsion force (i_x) are shown. They relate with i_d and i_q as mentioned in (15) and (16).

B. Motion quality experiment.

In this part of experiment, a test was carried out to check the effect of x-axis control to the two others. At the beginning the vehicle is controlled to stay in the middle of the guideway at position $x^* = 100$. At $t = 0.1s$ reference position is set to $x^* = 700$. Fig. 11 and Fig. 12 show results of speed, delta, and gamma as a function of position. In Fig. 11 the vehicle was set to run at speed = 400mm/s and in Fig. 12 was 600mm/s. The results show that the speed of the vehicle

affects the quality of delta and gamma control. The higher speed causes the lower quality of delta and gamma control. As shown in Fig. 11 and Fig. 12, the delta and gamma signals vibrate more when the vehicle moves through junction point of two segments (position=380mm). This is the result of the reduced magneto motive force (MMF) in the first and last pole of each stator, due to lacking windings [16] at this area.

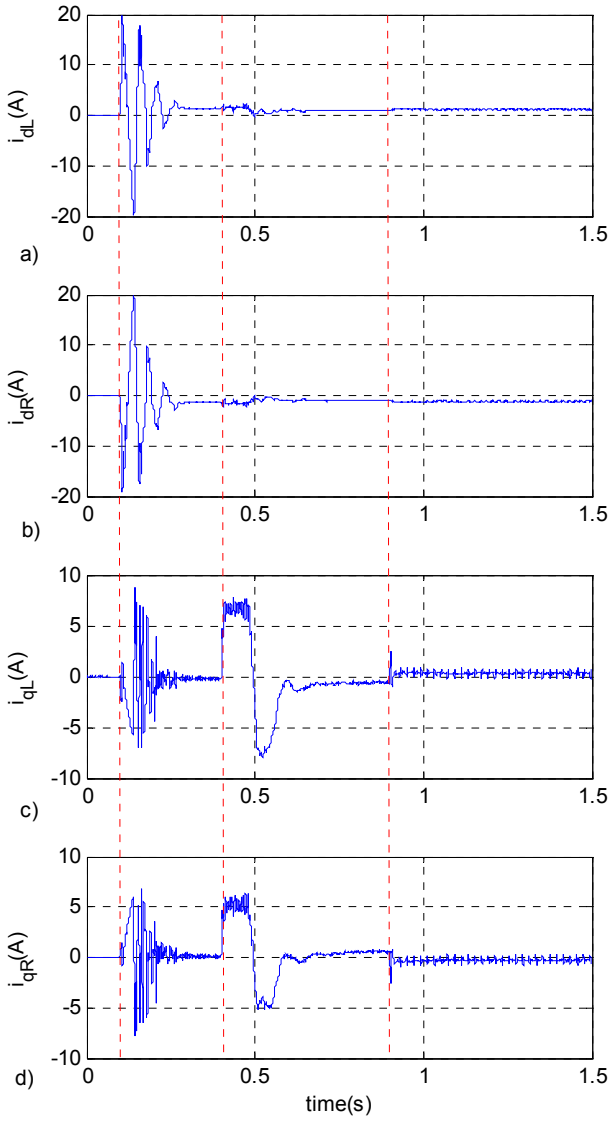

Fig. 7. Field oriented control current i_d, i_q of left and right side without compensation.

As mentioned before, only the segment or the two segments that have the vehicle moving above are supplied from the inverters. The others are in standby mode. Fig. 13 shows the currents of segment 1 and 2. The currents of segment 2 are provided only when the vehicle starts to move into the segment (at position = 260 mm). The currents of segment 1 are cut off to zero when the vehicle gets out of the segment (at position = 500mm).

V. Conclusions

An active magnetic guidance for PM-synchronous linear motors with long primary was presented. Applications like in-plant transport and handling systems would specially profit from it. The use of active magnetic guidance for the lateral displacement and yaw angle, while keeping a mechanical guidance for the vertical displacement, simplifies the mechanical assembly significantly without higher complexity in electromagnetic actuators or control. The experimental results show the viability of the proposed system and its control algorithm.

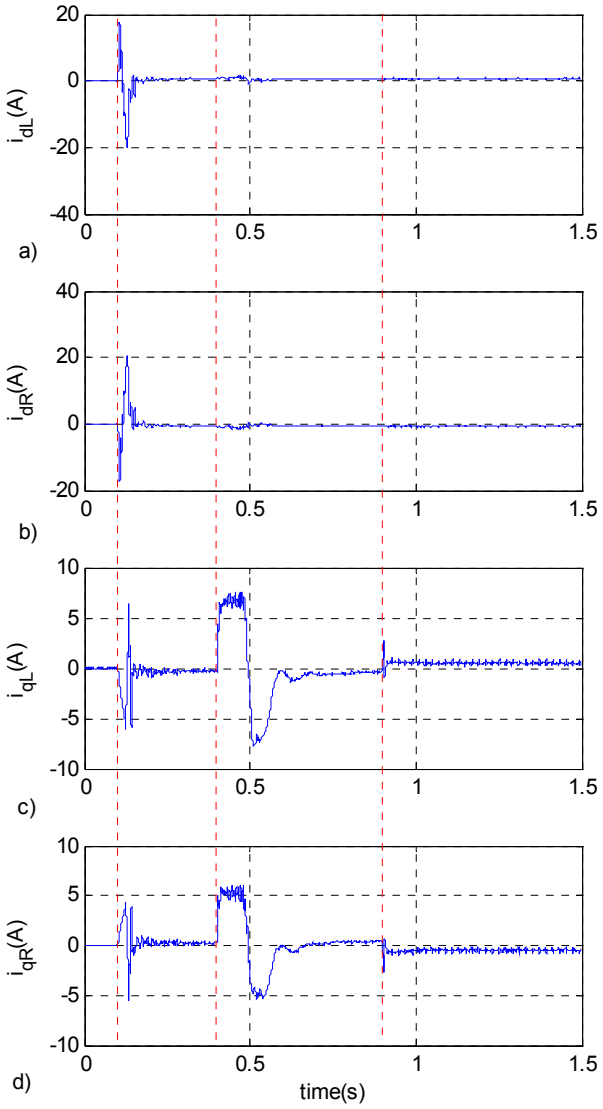

Fig. 8. Field oriented control current i_d, i_q of left and right side with compensation.

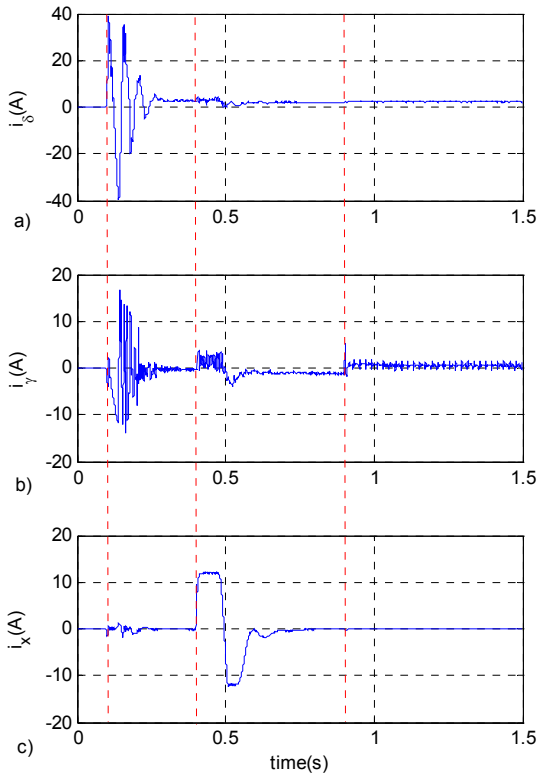

Fig. 9. The propulsion, lateral force and yaw torque-producing currents without compensation

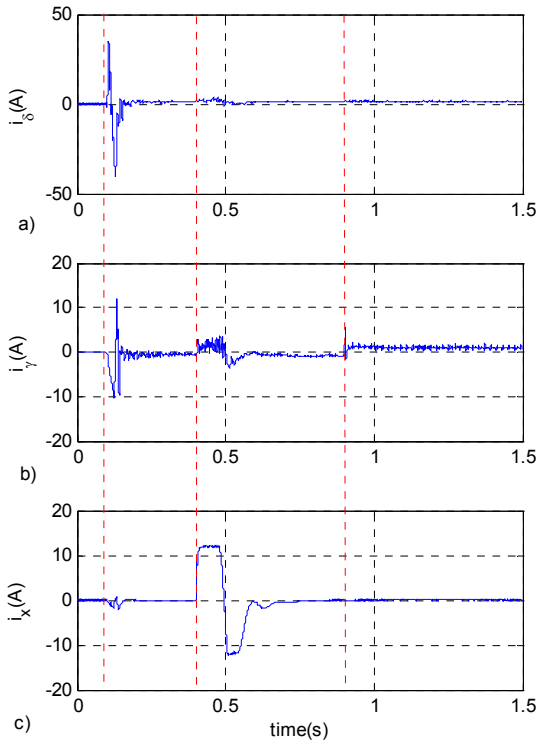

Fig. 10. The propulsion, lateral force and yaw torque-producing currents with compensation

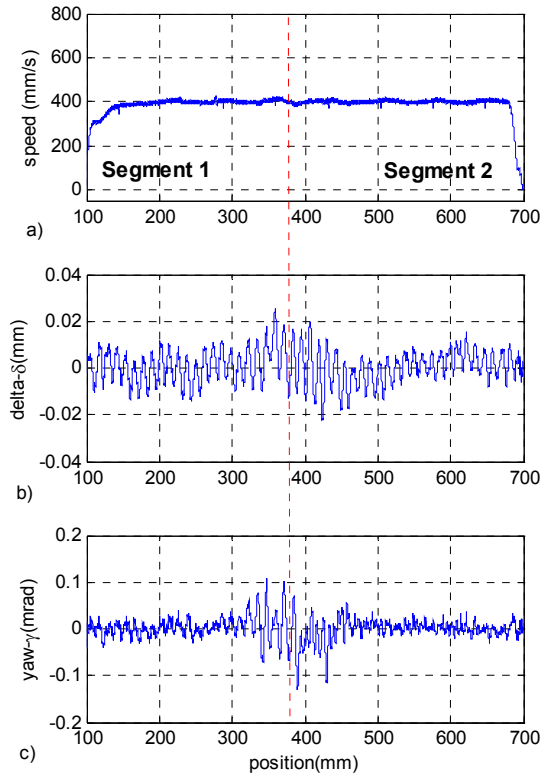

Fig. 11. The speed, delta, gamma of the vehicle as functions of position at speed = 400mm/s

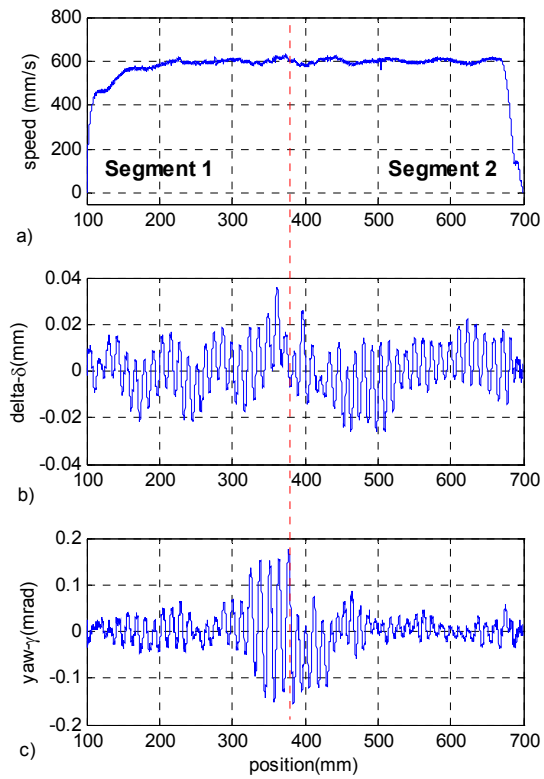

Fig. 12. The speed, delta, gamma of the vehicle as functions of position at speed = 600mm/s

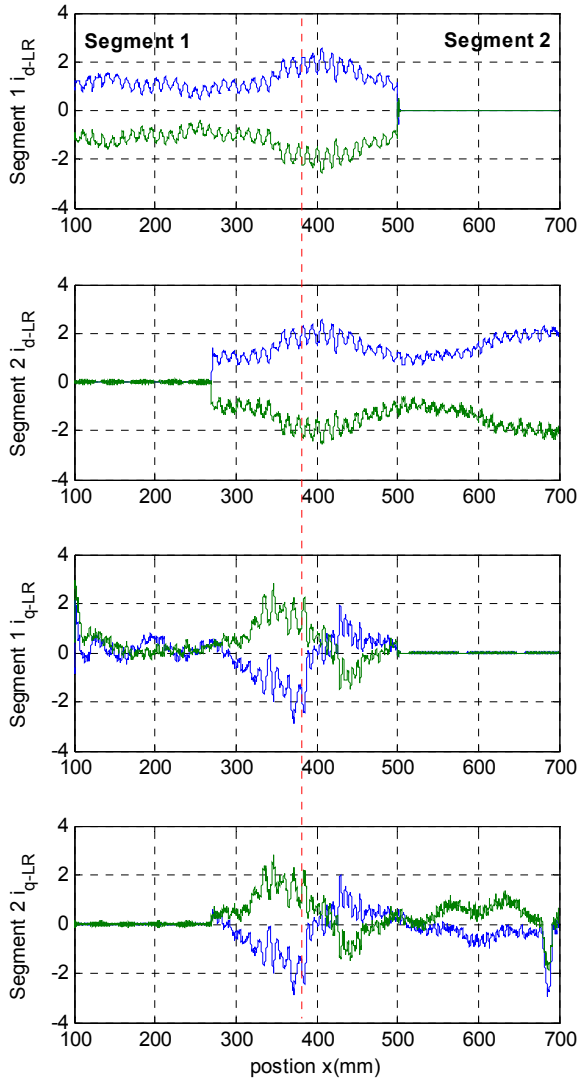

Fig. 13. Field oriented control current i_d, i_q of left and right side as the functions of position

REFERENCES

[1] B. Sieber, J. Breil, "New developments for a linear motor system with multiple carriers," in *Int. LDIA2003 Symp., 2003*, pp. 21-24.

[2] C. Bosshard, "MagneTrak(c) Paradigmenwechsel im Materialhandling," in *13. Deutscher Materialfluss-Kongress Innovative Techniken für die Logistik. vol. 1815 Garching, Germany,* 2004, pp. 189-200.

[3] G. Stöppler, "Segmentierte Langstator-Linearmotoren für die Schnellpositionierung von Werkstückträgern in längsverketteten Montagelinien," in *SPS/IPC/DRIVES/Electric Automation Systems and Components, Nuremberg, Gemany*, 2008.

[4] P. Mutschler, "Comparison of topologies for linear drives in industrial material handling and processing applications," in *7th Internatonal Conference on Power Electronics,* 2007. ICPE '07., 2007, pp. 1027-1032.

[5] J. de Boeij, M. Steinbuch, and H. M. Gutierrez, "Modeling the electromechanical interactions in a -flux electrodynamic maglev system," *IEEE Trans. on Magnetics, vol. 41,* pp. 466-470, 2005.

[6] S.O. Siems, W.-R. Canders, "Experimental investigation of linear and rotatory HTSC bearings for industrial applications," Int. *Journal of Applied Electromagnetics and Mechanics, vol. 19,* pp. 199-202, 2004.

[7] K. Ben-Yahia, G. Henneberger, "Linear magnetic bearing for high speed machine tools," in *PCIM 99 Nürnberg, 1999.*

[8] W. Evers, G. Henneberger, "A New Linear Drive for a Magnetic Levitation Transport System," in *EPE 99 Lausanne, 1999.*

[9] A. D'Arrigo, A. Rufer, "Design of an integrated electromagnetic levitation and guidance system for SwissMetro," in *EPE 99 Lausanne, 1999.*

[10] I. da Silva and O. Horikawa, "Experimental development of a one-degree-of-freedom controlled magnetic linear bearing," *IEEE Trans. on Magnetics, vol. 41,* pp. 4257-4260, 2005.

[11] K. Yoshida, T. Yoshida, K. Noda, "Combined-Levitation-and-Propulsion Control of SLIM Maglev Vehicle on Flexible Guideway," in *EPE 2003 Toulouse, 2003.*

[12] K. Yoshida, T. Yoshida, S. Manabe, and T. Yorishige, "Control of New PM LSM Maglev Vehicle Based on Analysis of Pitching Torque and Propulsion Force," in *IEEE Int. Symposium on Industrial Electronics, 2007. ISIE 2007, 2007,* pp. 1125-1130.

[13] I. Boldea, S.A. Nasar, *Linear electric actuators and generators*. Cambridge; New York: Cambridge University Press, 1997

[14] D. Schröder, *Elektrische Antriebe - Regelung von Antriebssystemen*, 3. ed Berlin, Heidelberg: Springer Berlin Heidelberg, 2009.

[15] R. Benavides and P. Mutschler, "Controlling a System of Linear Drives," in *Proc. Power Electronics Specialists Conference, 2005. PESC '05. IEEE 36th, 2005*, pp. 1587-1593.

[16] R. Benavides and P. Mutschler, "Compensation of Disturbances in Segmented Long Stator Linear Drives using Finite Element Models," in *Proc. Industrial Electronics, 2006 IEEE International Symposium on, 2006,* pp. 2445-2449.

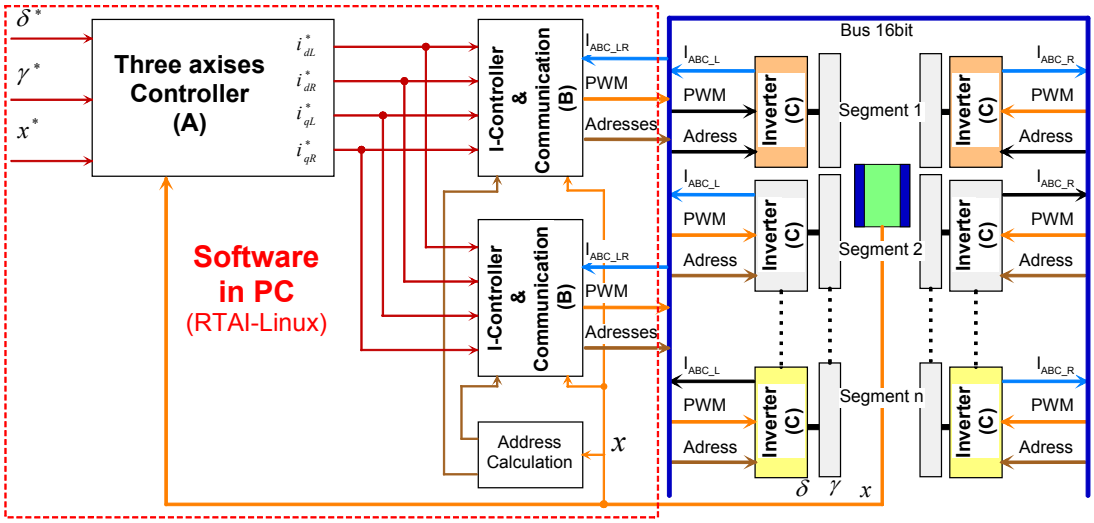

Fig. 14. Experiment Setup